

## Article

# Evaluation of the Effect of Particle Size and Biomass-to-Water Ratio on the Hydrothermal Carbonization of Sugarcane Bagasse

Leidy Natalia Moreno-Chocontá, Alejandra Sophia Lozano-Pérez \*  and Carlos Alberto Guerrero-Fajardo

Departamento de Química, Universidad Nacional de Colombia, Bogotá 111321, Colombia; lmorenoch@unal.edu.co (L.N.M.-C.); caguerrero@unal.edu.co (C.A.G.-F.)

\* Correspondence: aslozanop@unal.edu.co

**Abstract:** The generation of platform chemicals and hydrochar is of great interest because they reduce dependence on fossil resources and contribute to climate change mitigation by reducing carbon emissions. The main objective of this study was to evaluate the effect of biomass particle size and biomass-to-water ratio in a hydrothermal conversion system for the generation of value-added products obtained from sugarcane bagasse. Biomass characterization was performed using proximal, elemental, and structural analysis; hydrothermal carbonization was carried out at 220 and 260 °C for one hour; and conversion was monitored using pH, conductivity, and IR spectroscopy. Platform chemicals were quantified using HPLC-IR. Hydrochars were characterized by using scanning electron microscopy and energy dispersive spectroscopy. Optimizing biomass particle size and water ratio is crucial for maximizing the yield of platform chemicals and hydrochar. The study's outcomes revealed that specific combinations, such as a biomass-to-water ratio of 1:50 and a particle size of 212 µm at 220 °C, resulted in a substantial 31.07% yield of platform chemicals on a dry basis. This highlights the critical role these parameters play in influencing the production efficiency of valuable chemicals. Furthermore, variations in biomass particle size and water ratio also affect the characteristics of hydrochar. For instance, utilizing a biomass-to-water ratio of 1:50 and a larger particle size of 600 µm at 260 °C led to the production of hydrochar with higher carbon content and increased porosity. These findings underscore how adjustments in these factors can impact not only chemical yields, but also the properties and quality of the resulting hydrochar.

**Keywords:** hydrothermal carbonization; platform chemicals; hydrochar; sugarcane bagasse



**Citation:** Moreno-Chocontá, L.N.; Lozano-Pérez, A.S.; Guerrero-Fajardo, C.A. Evaluation of the Effect of Particle Size and Biomass-to-Water Ratio on the Hydrothermal Carbonization of Sugarcane Bagasse. *ChemEngineering* **2024**, *8*, 43. <https://doi.org/10.3390/chemengineering8020043>

Academic Editor: Dmitry Yu. Murzin

Received: 17 February 2024

Revised: 6 March 2024

Accepted: 22 March 2024

Published: 8 April 2024



**Copyright:** © 2024 by the authors. Licensee MDPI, Basel, Switzerland. This article is an open access article distributed under the terms and conditions of the Creative Commons Attribution (CC BY) license (<https://creativecommons.org/licenses/by/4.0/>).

## 1. Introduction

Because of the depletion and environmental issues caused by the use of fossil fuels, renewable raw materials have become the preferred option for many material and energy needs. Thus, biomass presents itself as an interesting option, as it is the most abundant organic material on Earth. Colombia has favorable agroclimatic conditions for establishing agro-industrial activity [1]. Sugarcane is one of the most productive and widely used crops in the country, and it is used to make refined sugar, panela, and bioethanol. Sugarcane production is the country's second-largest agricultural industry generating around 16.5 million tons of bagasse each year [2–4]; approximately 70% of the unprocessed raw material becomes waste products [4,5]. For this reason, it is important not only to provide food security for the population, but also to recover waste and reduce its environmental impact [6,7].

Hydrothermal treatments are appropriate and efficient systems for the conversion of wet biomasses. Under hydrothermal conditions, water favors reaction mechanisms that break down the cellulose, hemicellulose, and lignin present in the biomass [8]. In this sense, hydrothermal carbonization (HTC) is a thermochemical process that consists of the conversion of biomass by the action of an aqueous reaction medium, in which hydrolysis is favored by ionization reactions. The system conditions should range from 180 to 260 °C and 1 to 5 MPa where the water stays in its liquid state [9].

The products obtained in hydrothermal carbonization systems carried out at 180 °C, are a wide variety of water-soluble platform chemical, such as monomeric sugars (glucose, xylose, galactose, and arabinose, among others) [10], products of the hydrolysis of cellulose and hemicellulose. On the other hand, at temperatures above 200 °C, monomers can produce new compounds such as 5-hydroxymethyl-2-furfural and fructose [11]. Other reaction mechanisms, such as dehydration, decarboxylation, condensation, polymerization, and aromatization, can occur simultaneously. Dehydration and decarboxylation of HMF and furfural derivatives can produce acetic acid, formic acid, levulinic acid, aldehydes, water, and gaseous products such as carbon dioxide. Also, polymerization reactions by aldol condensation and aromatization produce a lignite-like solid called a hydrochar [11–13].

Platform chemicals have different applications in the industry of additives, solvents, reagents, and lubricants, among other products of high commercial value [14]. While hydrocarbons are currently under study, it has been demonstrated that these carbonaceous materials have a wide variety of applications. Some of these include catalyst supports, bio-fuels, activated carbon and adsorbent materials for wastewater treatment, soil remediation, CO<sub>2</sub> sequestration, and some other applications [15,16].

Studying the particle size of biomass and the biomass-to-water ratio in hydrothermal carbonization (HTC) processes is essential due to their significant impact on the efficiency and outcomes of the conversion system. Understanding how these factors influence the production of platform chemicals and hydrochar from biomass sources like sugarcane bagasse is crucial for optimizing the process and maximizing the yield of value-added products [17]. The particle size directly affects the surface area available for reactions, influencing reaction kinetics and mass transfer rates within the system. On the other hand, the biomass-to-water ratio plays a key role in determining the solubility of biomass components, affecting the overall conversion efficiency and product quality. By studying and optimizing these parameters, researchers can fine-tune HTC systems to achieve higher yields of platform chemicals and high-quality hydrochar while reducing reliance on fossil resources and contributing to sustainable practices in chemical production [18].

The novelty of this study lies in its focus on evaluating the effect of biomass particle size and biomass-to-water ratio on the hydrothermal conversion process for generating value-added products from sugarcane bagasse. This research contributes to the existing literature by providing valuable insights into optimizing these parameters to enhance the efficiency of platform chemicals and hydrochar production [19]. In contrast to other articles, this study offers a more comprehensive understanding of how biomass particle size and water ratio influence the hydrothermal conversion process. For instance, the study by Oktaviananda et al. (2017) [20] discusses the production of hydrochar from biomass, but does not focus on the effect of biomass particle size. Different studies assess the potential use of hydrochar from sugarcane industry by-products as a soil conditioner, but it does not delve into the effect of biomass particle size and water ratio on the hydrothermal conversion process. The life cycle assessment of electricity generation from sugarcane bagasse hydrochar produced by microwave-assisted hydrothermal carbonization in Fregolente et al. (2021) [21] provides environmental impact insights, but does not specifically address the influence of biomass particle size and water ratio on the hydrothermal conversion process.

This study is expected to contribute to the optimization of the conversion parameters of an HTC reaction system for the valorization of sugarcane bagasse from the Colombian industry. In order to achieve that, the yields of the products obtained from the optimization of the parameters (particle size of the raw material and B:W ratio of the system) at two working temperatures were determined. The results obtained are expected to be a basis for future research, with the objective of achieving higher yields in the products and thus increasing their value in the agro-industrial production chain.

## 2. Materials and Methods

### 2.1. Sampling of Residual Biomass

The biomass selected for this research was sugarcane bagasse. In total, 2 kg of this raw material was donated by a producer associated with the National Federation of Panela Producers (Fedepanela). The sampling was carried out on a farm in the municipality of La Peña, Cundinamarca, in the province of Gualivá, located 140 km northwest of Bogotá. Biomass was collected fifteen days after milling.

### 2.2. Sugarcane Bagasse Primary Pretreatment

The primary pretreatment of the biomass was performed in accordance with the 2008 technical report NREL/TP-510-42620 [22], "Preparation of samples for compositional analysis". This technical standard describes how to convert the biomass sample into a material suitable for reproducible analysis and processing. The pretreatment applied to this biomass was grinding and sieving. The grinding process was carried out in a SM100 cutting mill with a 1 mm-diameter screen. This mill has a parallel cutting rotor that passes close to the sieve ring, crushing the particles through the collision of the rotating cutting disc, shear forces, and friction exerted by the sieve ring and rotor blades on the particles. After grinding, sieving was carried out with sieves meeting specifications (600, 212 y 106  $\mu\text{m}$ ).

### 2.3. Biomass Characterization Techniques

#### 2.3.1. Proximal Analysis

Proximal analysis includes the determination of moisture, ash, volatile matter, and fixed carbon content. The laboratory analytical procedures used correspond to: moisture NREL/TP-510-42621 [23], March 2008; and "Determination of total solids in biomass and total dissolved solids in process liquid samples", ash NREL/TP-510-42622 [24], January 2008. "Determination of ash in biomass", volatile matter ASTM E872-82, 2019 [25], "Standard test method for volatile matter in wood fuel particulate analysis". Fixed carbon was calculated as  $100 - (\% \text{moisture} + \% \text{volatile matter} + \% \text{ash})$ .

#### 2.3.2. Ultimate Analysis

Based on the ASTM-D5373 [26] analytical procedure, the raw material underwent elemental analysis. The purpose of this analysis is to determine the percentage of carbon, hydrogen, nitrogen, sulfur, and elemental oxygen; the latter was determined by the difference in its elemental composition.

#### 2.3.3. Structural Analysis

This analysis was used to determine the cellulose, hemicellulose, and lignin content present in the sugarcane bagasse based on the protocols FNA-AOAC 973.18 [27], "Official methods of analysis, acid detergent fiber", FND-AOAC 200.04 [28], "Official methods of analysis, neutral detergent fiber", and Lignin-AOAC 973.18 [27], "Official methods of analysis, lignin", respectively.

### 2.4. Hydrothermal Treatment of Biomass

The choice of temperatures at 220 °C and 260 °C and biomass-to-water ratios of 1:10 and 1:50 in the hydrothermal conversion (HTC) experiments was based on specific considerations. A preliminary scan was conducted to identify the optimal conditions for conductivity and pH within the HTC range, leading to the selection of 220 °C as the temperature that exhibited the highest conductivity and lower pH, indicating favorable reaction conditions. This temperature was deemed most suitable for biochar production, aligning with previous research indicating its efficacy in the hydrothermal treatment of biomass.

Research indicates that different biomass-to-water ratios can significantly impact the yield and properties of hydrochar produced from biomass. By comparing ratios like 1:10 and 1:50, researchers can determine the most effective concentration that maximizes product

yields and quality while ensuring efficient utilization of resources. Moreover, the selection of these specific ratios aligns with previous studies that have highlighted the importance of optimizing biomass-water ratios for HTC processes. Research has shown that variations in biomass-to-water ratios, within the range of 5–20%, can have a substantial effect on the outcomes of hydrothermal treatment, emphasizing the need to carefully evaluate and select the most suitable ratio for desired product characteristics. By focusing on ratios like 1:10 and 1:50, this study aims to contribute valuable insights into the impact of biomass concentration on the HTC process, aiming to enhance efficiency, maximize product yields, and promote sustainable practices in chemical production.

The hydrothermal carbonization was carried out in a high-pressure synthesis batch reactor in stainless steel with a capacity of 500 mL. Twelve experiments were carried out at two temperatures, 220 and 260 °C, with self-generated pressure, residence time 1 h, biomass-to-water ratio, and particle size parameters were varied. To evaluate the biomass-to-water ratio influence, 1:10 and 1:50 ratios were taken; for the 1:10 ratio, 10 g of dry biomass per 100 g of water were taken; and for 1:50 ratio, about 5 g of biomass on a dry basis per 250 g of water were weighed; the sizes used to compare the particles' size influence were: small (106 µm), medium (212 µm), and large (600 µm).

Table 1 shows the experimental design implemented. The fractions of the reactions were vacuum filtered, and two products were obtained: an aqueous phase and a solid phase.

**Table 1.** Experimental design evaluation of parameter B:W ratio and particle size.

Experiment	Temperature (°C)	Biomass-to-Water Ratio B:W	Particle Size (µm)
1	220	1:10	106
2	260	1:10	106
3	220	1:50	106
4	260	1:50	106
5	220	1:10	212
6	260	1:10	212
7	220	1:50	212
8	260	1:50	212
9	220	1:10	600
10	260	1:10	600
11	220	1:50	600
12	260	1:50	600

#### 2.4.1. Aqueous Phase

The pH and conductivity from the aqueous phase were measured to monitor the formation of acidic compounds characteristic of the decomposition of lignocellulosic biomass. The equipment used to measure these properties was a Hanna Instruments pH and conductivity meter reference HI-HI5522.

#### Identification and Quantification of the Formation of Platform Chemicals

The aqueous products were analyzed using High Performance Liquid Chromatography (HPLC) on a Hitachi LaChrom Elite® HPLC System by Hitachi High Technologies America. Characteristics of the chromatographic method: stationary phase: Shodex, Sugar SH1821 8.0 × 300 mm, particle size: 6 µm; mobile phase: 0.005 M sulfuric acid solution, flow rate 0.5 mL/min; column temperature: 60 °C, injection volume 20 µL; method run time 60 min; and detection system: Hitachi RI (Refractive Index) L-2490 detector. The standards used for the determination of the platform chemicals obtained from the HTC treatment applied to sugarcane bagasse were glucose, xylose, formic acid, levulinic acid, HMF, and furfural. Finally, with Equation (1), the performance of the platform chemicals was determined.

$$\text{Yield of aqueous products (wt\%)} = \left( \frac{\text{mass of liquid products (g)}}{\text{biomass mass on dry (g)}} \right) * 100 \quad (1)$$

#### 2.4.2. Solid Phase (Hydrochar)

The solid was dried at 105 °C to a constant weight, then analyzed using infrared spectroscopy using the ATR analysis method, Nicolet iS10 Spectrometer, Thermo Fisher Scientific equipment, MA, USA, to study and follow up on the breakdown of the characteristic chemical bonds in the sugarcane bagasse. To characterize the hydrocarbons, the morphology was evaluated by means of a scanning electron microscope, Bruker Nano GmbH Berlin, Germany, VEGA 3 TESCAN Easy Probe. The elemental composition of the hydrocarbons was also determined by energy dispersive spectroscopy with an X-ray detector (EDX). In addition, Equation (2) was used to determine the percent biomass conversion rate.

$$\text{Conversion percent of dry solid products (wt\%)} = \left( \frac{\text{mass of dry biomass} - \text{mass of solid product.}}{\text{mass of dry biomass}} \right) * 100 \quad (2)$$

### 3. Results

In the conversion of sugarcane bagasse, the biomass, water, and particle size ratio parameters were evaluated at various temperatures. The goal is to identify and describe the conditions that result in higher yields in the production of value-added products through the hydrothermal carbonization process.

#### 3.1. Biomass Characterization

##### 3.1.1. Proximal Analysis

Table 2 shows the results of the proximal analysis of sugarcane bagasse and data from other biomasses reported in the literature. The percentage of moisture refers to the water content present in the biomass. The sugarcane bagasse has 7.910% moisture; the value obtained is comparably close to that reported for another sample of sugarcane bagasse, whereas, when compared to other biomasses, this is a source with a high moisture content. This is a great advantage, because the high moisture content represents energy savings during the primary pretreatment, avoiding drying prior to the biomass conversion process, and it also reduces the amount of water needed to carry out the hydrothermal reaction system.

**Table 2.** Proximal analysis of the sugarcane bagasse compared to other biomasses.

Ref.	Biomass	% Moisture	% Ash	% Volatile Matter	% Fixed Carbon
Sample	Sugarcane bagasse <sup>1</sup>	7.910 ± 0.07	1.556 ± 0.02	80.93 ± 0.09	9.601
[22]	Sugarcane straw <sup>2</sup>	0.90	9.60	77.25	13.31
[23]	Sugarcane bagasse <sup>2</sup>	7.32	4.76	83	12.9
[24]	<i>Pennisetum</i> pasture <sup>2</sup>	8.17	10.73	73.44	15.83

<sup>1</sup> Obtained result in the sample; <sup>2</sup> results were reported for other biomasses.

The proportion of ash indicates the amount of minerals and inorganic compounds that are not combustible. Sugarcane bagasse thus contains 1.556% inorganic and mineral compounds following combustion. This raw material is found to have a low ash content when compared to other biomasses and another sample of sugarcane bagasse. Compared to raw materials with a higher percentage of ash, lignocellulosic biomass with a lower percentage of ash is thought to be a more advantageous raw material for thermal conversion processes like pyrolysis, combustion, and gasification because it will result in a lower formation of inorganic solid residues. Conversely, a lower production of inorganic solid residues is seen as advantageous, since it lessens the harm that residue generation causes to the environment and can help create biofuels that are more sustainably produced and efficient [29].

The percentage of volatile matter in the sample indicates how much condensable and non-condensable gaseous products are released during heating. Table 2 shows that the percentage of volatile matter in bagasse made from sugarcane is 80.932%. This number is within the range of information that has been published in other studies. Because of its high volatile matter content, the biomass burns quickly, producing a variety of combustible gaseous, liquid, and solid products. On the other hand, fixed carbon represents the portion of solid carbon that is left over after biomass is burned. This type of carbon is made up of the elemental carbon that remains after volatile matter decomposes, and is found in biomass and other carbonaceous compounds. Stated differently, the percentage of fixed carbon is a variable quantity because it depends on the formation products of the volatile matter as well as the rate of heating [30].

However, the formation of fixed carbon, which is measured by counting the percentage of volatile matter under controlled conditions, is one parameter that provides information about the combustion of the biomass. Table 2 demonstrates that bagasse derived from sugarcane has the lowest percentage of fixed carbon (9.601%), indicating that the amount of solid product produced by this raw material is less than that of other biomasses [31,32].

### 3.1.2. Ultimate Analysis

The elemental composition of sugarcane bagasse is shown in Table 3 as follows: 45.22% carbon, 5.94% hydrogen, 0.292% nitrogen, and 48.56% oxygen. There is no sulfur content. We can see that this biomass's elemental composition falls between the average range of other lignocellulosic residual biomasses. Regarding composition, bagasse's low nitrogen and sulfur-free levels make it appropriate for use in thermochemical conversion processes like hydrothermal, as these low concentrations lessen the production of greenhouse gases and other harmful gases like sulfur oxides and nitrogen [33–35].

**Table 3.** Elemental analysis of the biomass sample compared to other biomasses.

Ref.	Biomass	% C	% H	% N	% O	% S
Sample	Sugarcane bagasse <sup>1</sup>	45.22	5.94	0.292	48.56	0
[22]	Sugarcane straw <sup>2</sup>	44.80	5.94	0.10	48.89	0.27
[29]	Sugarcane bagasse <sup>2</sup>	46.2	5.9	0.21	47.5	-
[31]	Rice shell <sup>2</sup>	40.82	5.25	0.38	53.38	0.17

<sup>1</sup> Obtained result in the sample; <sup>2</sup> results were reported for other biomasses.

### 3.1.3. Structural Analysis

Details about the structural makeup of sugarcane bagasse are shown in Table 4. According to the data, this raw material has a higher cellulose percentage (61.4%) than other biomasses that have been reported, and its hemicellulose content (23.6%) is consistent with other samples made from sugarcane bagasse and other biomasses that have been reported in the past. However, lignin (8.1%) comprises less of this raw material than all the other biomasses.

**Table 4.** Structural analysis of the biomass sample in comparison with other biomasses.

Ref.	Biomass	% Cellulose	% Hemicellulose	% Lignin
Sample	Sugarcane bagasse <sup>1</sup>	61.4	23.6	8.1
[33]	Sugarcane straw <sup>2</sup>	50.81	20.36	9.18
[32]	Sugarcane bagasse <sup>2</sup>	45.28	22.13	22.39
[27]	Sugarcane bagasse <sup>2</sup>	35.28	33.25	25.20

<sup>1</sup> Obtained result in the sample; <sup>2</sup> results were reported for other biomasses.

Because they boost the conversion of value-added products, sugarcane bagasse's high cellulose and hemicellulose contents imply that it is the ideal raw material to use in the HTC process. It is anticipated that under the HTC conversion system's operating conditions,

cellulose and hemicellulose will hydrolyze to fermentable sugars. These sugars can then serve as precursors in other reaction mechanisms to produce chemical compounds with a broad range of applications, including furfural derivatives and organic acids.

This raw material's low lignin content, when compared to the other structural components of the biomass and the lignin percentage in other samples mentioned in Table 4, is a significant advantage in terms of the yield of products derived from cellulose and hemicellulose. It is well known that lignin is more resistant to heat breakdown; however, because it makes up a smaller portion of the structure, its impact on the conversion process is lessened. Similarly, the fragmentation of the sample and its reduced lignin content make it suitable for effective HTC conversion processes. This is because fragmentation increases the surface area of the particles, which in turn increases access to the structural components. Therefore, the milling process indirectly affects the conversion of the biomass's structural components.

### 3.2. Hydrothermal Treatment of Biomass

#### 3.2.1. Aqueous Phase

##### Conductivity Monitoring, pH Measurement, and Particle Size Variation

Particle size and biomass-to-water ratio are fundamental parameters that exert a significant influence on the product yields and properties in hydrothermal valorization processes. Research studies by Heidari et al. (2018) have highlighted the critical role of these factors in shaping the efficiency and outcomes of the conversion process [27,36]. Specifically, smaller particle sizes have been associated with enhanced reaction kinetics, facilitating increased conversion efficiency and higher product yields. Moreover, higher biomass-to-water ratios have been shown to improve mass transfer rates within the system, ultimately impacting the overall process efficiency [37]. The solubility of biomass components is intricately linked to the biomass-to-water ratio, with optimal ratios leading to improved conversion efficiency and superior product quality [38]. Additionally, the interplay between particle size and biomass-to-water ratio influences heat and mass transfer rates, further underscoring their importance in optimizing hydrothermal valorization processes [39]. Notably, these factors not only affect product yields, but also play a crucial role in determining the properties of the final products, such as hydrochar [40]. Studies have demonstrated how variations in particle size and biomass-to-water ratio can impact key characteristics of hydrochar, including carbon content, porosity, and heating value [41]. By meticulously adjusting these parameters based on empirical data and scientific insights, researchers can fine-tune hydrothermal valorization processes to achieve maximal product yields and quality while advancing sustainable practices in chemical production [42].

To monitor the evolution of the pertinent compounds generated in the liquid phase, measurements of pH and conductivity were made. Consequently, a plot of the conductivity and pH results is displayed in Figure 1. First, the difference in conductivity was found to be approximately one unit throughout the whole data set, and the variation in pH was found to be less than one unit based on the data displayed by the pH graph. Based on the findings, it was clear that sugarcane bagasse tends to produce more  $H^+$  ions at 600  $\mu\text{m}$  than at 106 and 212  $\mu\text{m}$  when compared to treated biomass. Similar trends could also be seen in the conductivity graph, where an increase in conductivity values was seen for reaction operating parameters carried out with a 600  $\mu\text{m}$  size. Possibly this is since small particle sizes can favor different reaction mechanisms with the medium, such as polymerization due to the increase in the surface area of the particle, which leads to a lower formation of acidic species in the aqueous medium [19,40].

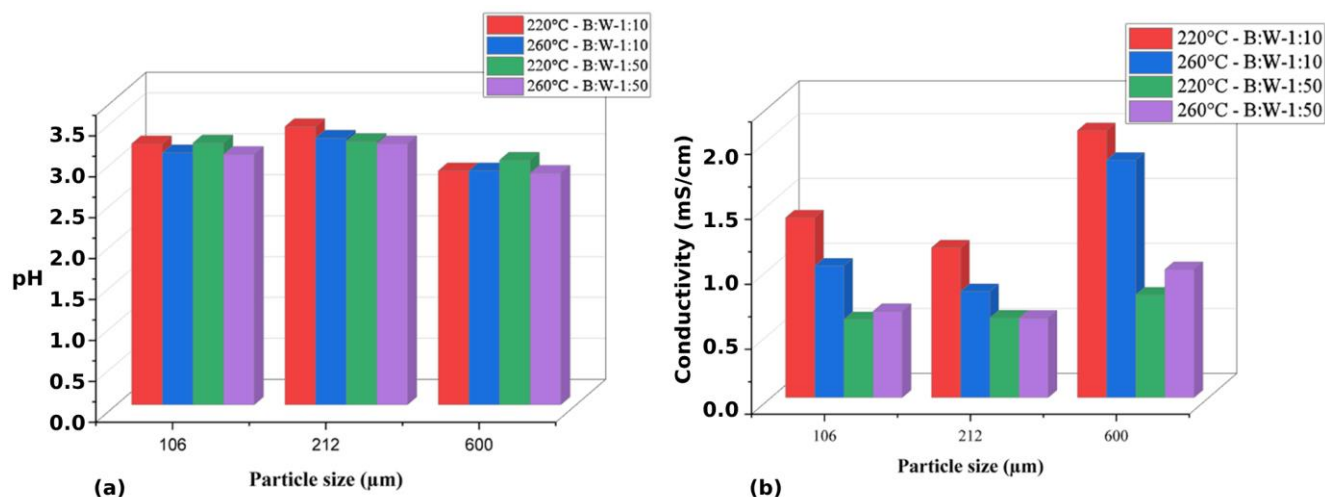


**Figure 1.** HTC reaction tracking using (a) pH; (b) conductivity with respect to particle size variation.

#### Experiments with B:W Ratio Variation, pH, and Conductivity Monitoring

In Figure 2, the variation of the concentration of acid species as a function of the B:W ratio was analyzed. In the pH graph (a), the two B:W ratios (1:10 and 1:50) show that the conditions with the highest concentrations of  $H^+$  acidic species are particle sizes of 600  $\mu\text{m}$  at temperatures of 220 and 260  $^{\circ}\text{C}$ . Likewise, in the measurement of conductivity (number b) in this same figure, it is found that for the two B:W ratios, the parameters that present higher conductivities are the particle size of 600  $\mu\text{m}$  in both temperatures of 220  $^{\circ}\text{C}$  and 260  $^{\circ}\text{C}$  and ratios of 1:10 and 1:50.

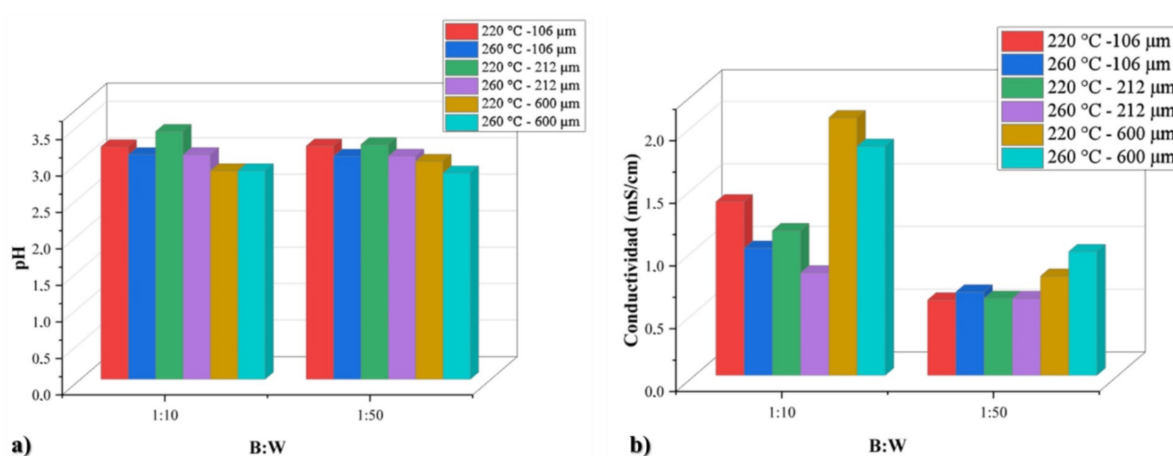


**Figure 2.** Tracking of the HTC reaction using (a) pH; (b) conductivity with respect to the variation in the B:W ratio.

#### Quantification of Platform Chemicals

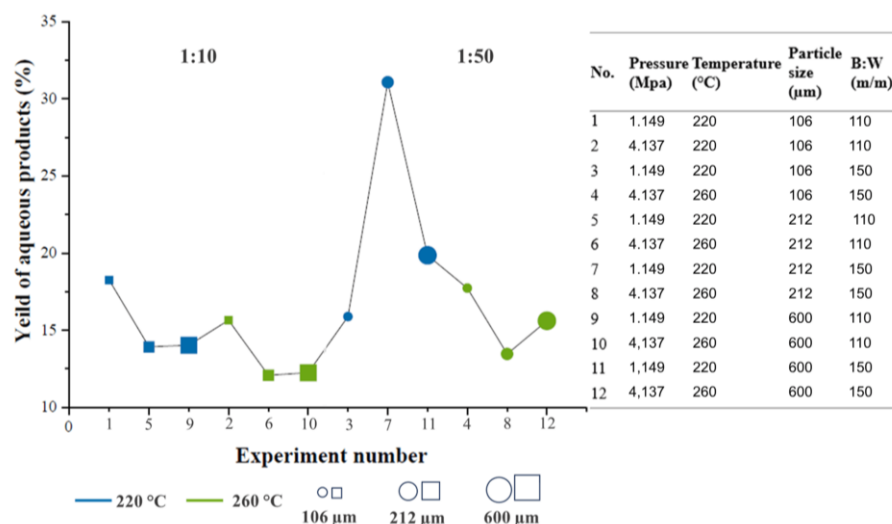
The results of the yields of the platform chemicals obtained in the aqueous phase are recorded in Table 5. In this table, the concentrations of the platform chemicals were recorded to determine the total yield of the products in the aqueous phase.

Figure 3 shows the yields of the aqueous fractions. It is observed that in experiment 7, the best yield in weight of the aqueous products was obtained (31.073%). The conditions of said experiment were a B:W ratio of 1:50, a temperature of 220  $^{\circ}\text{C}$ , and a particle size of 212  $\mu\text{m}$  (as presented in the Materials and Methods section). When comparing the effect of particle size with the results obtained, it was observed that the experiments performed with a B:W ratio of 1:10 produce better yields when the particle size of 106  $\mu\text{m}$  was used (18.25 and 15.65% at 220  $^{\circ}\text{C}$  and at 260  $^{\circ}\text{C}$ , respectively). This is because smaller particle sizes undergo higher conversions because reducing the size of the biomass favors a

greater diffusion of water in the biomass, which results in a faster decomposition of the lignocellulosic material, resulting in a decrease in yields [13,34].

**Table 5.** Yield of platform chemicals aqueous fraction.

Experiment Number	Concentration (g/L)					%
	Carbohydrates	Formic Acid	Levulinic Acid	HMF	Furfural	
1	0.685	4.854	9.306	2.014	2.547	18.253
2	0.334	6.326	9.413	0.007	0.000	15.654
3	0.115	1.274	0.597	0.559	0.661	15.880
4	0.148	2.724	0.780	0.000	0.000	17.729
5	0.316	8.348	3.635	1.277	0.941	13.926
6	0.347	7.894	3.838	0.000	0.000	12.082
7	0.232	2.991	0.758	0.970	0.884	31.072
8	0.157	4.18	0.983	0.025	0.000	13.463
9	0.820	6.049	3.531	3.051	2.600	14.028
10	0.301	7.920	3.961	0.000	0.705	12.247
11	0.222	1.657	0.718	0.812	0.714	19.857
12	0.069	2.309	0.791	0.000	0.000	15.608



**Figure 3.** Yield of liquid products in aqueous phase.

Likewise, in the ratio B:A 1:50 at 260 °C, it was observed that the particle size of 106 μm has a higher yield (17.73%) compared to the other two particle sizes. On the contrary, in the experiments carried out with the B:W ratio of 1:50, it was evidenced that at 220 °C, the best yields were reached with the largest particle sizes, 212 and 600 μm, compared to that of 106 μm (31.72; 19.85; 15.88%, respectively). When analyzing the effect of the B:W in the production of platform chemicals, it was observed that with the 1:50 ratio, it tends to increase the yield in comparison to the results obtained in the 1:10 ratio, since the amount of water is a key factor in guaranteeing the dispersion of the biomass in the reaction system, which results in a more efficient process [21,31].

Also, Figure 4 shows the percentage yield for each of the platform chemicals that constitute the total yield of the aqueous phase products. From the information provided by this graph, it was observed that formic acid is the chemical product with the highest formation from sugarcane bagasse under HTC conditions, followed by levulinic acid. According to what has been reported by other studies, cellulose and hemicellulose in a hydrothermal system are known to hydrolyze at temperatures above 180 °C [42]. However, when the reaction system reaches 220 °C, further decomposition of cellulose and hemicellulose occurs. This occurs through a hydrolysis reaction where the ester and ether bonds (mainly

the O-glycosidic bond) are broken to produce soluble oligomers such as saccharides and monosaccharides. Sugarcane bagasse is known to contain mainly glucose, galactose, xylose, and arabinose [43–45].

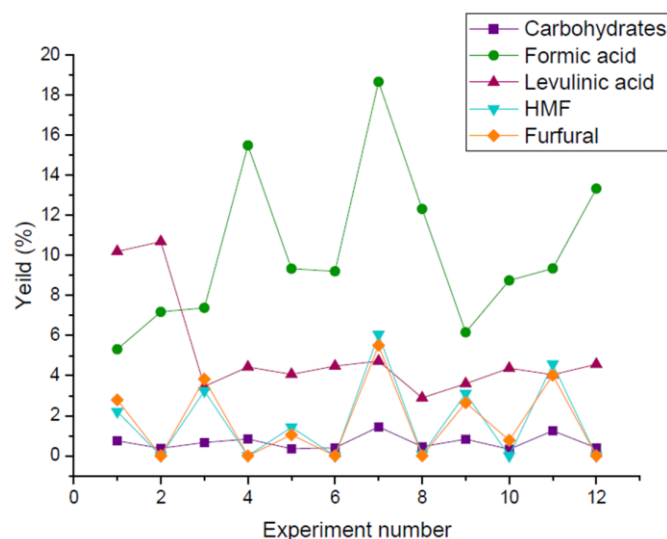


**Figure 4.** Percentage yield for each of the platform chemicals.

### 3.2.2. Solid Phase (Hydrochar)

#### Infrared Spectroscopy

Infrared spectroscopy was done to see structural alterations in the lignocellulosic material's chemical composition. IR spectra of the untreated biomass and those found in the solid products of the hydrothermal treatment were compared in Figure 5. The unaltered biomass is represented by the gray spectrum. Owing to the material's heterogeneity, numerous distinguishing peaks of the bonds pertaining to the biopolymers that make up the lignocellulosic biomass were visible. Thus, the cellulose, hemicellulose, and lignin bond characteristic peaks were found in the fingerprint region and are as follows ( $\text{cm}^{-1}$ ): 666.33–833.12–1033.16–1158.91–1204.38–1315.47–1427.09–1453.05–1513.11–1603.94–1704.48.

The 666.33 and 832.12  $\text{cm}^{-1}$  bands may correspond to bending vibrations between the hydrogen–carbon bonds of the aromatic compounds of lignin, as well as vibrations of the (C-H) groups of the glycopyranose ring of cellulose and hemicellulose. The bands at 1033.16  $\text{cm}^{-1}$  are characteristic of the stretching vibration of the single (C-O) bonds present in the polysaccharides and oligosaccharides of cellulose and hemicellulose; these signals serve to describe the deformation of the (C-O) bonds of some primary alcohols and of the (C-H) bonds of polysaccharides and lignin [46,47]. The signal at 1158.91  $\text{cm}^{-1}$  describes the stretching vibrations of the glycosidic bonds in cellulose and hemicellulose (C-O-C). In addition, it is typical of the aliphatic bending of the (C-H) bond of the syringyl ring.

The absorption signal in the range of 1204.38  $\text{cm}^{-1}$  is caused by the stretching vibrations of the (C-O) bonds of aliphatic compounds, which may correspond to the oxygen-containing functional groups in cellulose and hemicellulose. The signal corresponding to the wavenumber 1315.47  $\text{cm}^{-1}$  corresponds to the stretching vibration of the aryl alkyl ester groups of the syringyl and condensed guaiacyl rings present in lignin (O-CH<sub>3</sub>); 1427.09 and 1453.05  $\text{cm}^{-1}$  are the characteristic signals of the asymmetric vibrations of aromatic groups of hemicellulose (CH, CH<sub>2</sub>, and CH<sub>3</sub>). At 1513.11 and 1603.94  $\text{cm}^{-1}$ , these signals may correspond to the vibrations and stretching of the bonds of the ketone groups of hemicellulose (C=O), as well as the vibrations of the bonds (C=C) belonging to the aromatic compounds. And at 1704.48  $\text{cm}^{-1}$  there are (C=O) stretches of ketones, carbonyls, unconjugated ester groups, and xylan acetates of hemicellulose [46,48]. As for the 3334.24 and 2916.21  $\text{cm}^{-1}$  signals, the first signal is characteristic of aliphatic (O-H) hydroxyl bonds,

while the other may correspond to (C-H) bond stretching of aliphatic hydrocarbons present in cellulose.

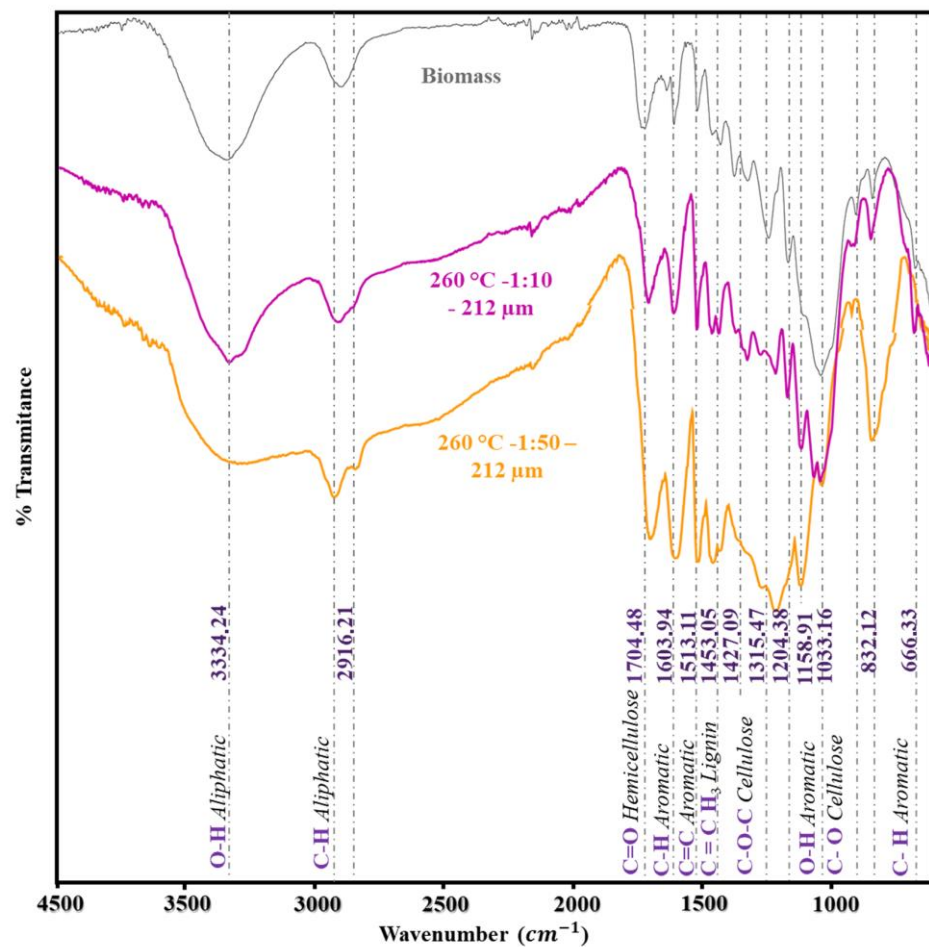


**Figure 5.** Comparison of structural changes in lignocellulosic material.

Comparing the spectra of experiments of ratio 1:10 y 1:50 to the untreated biomass levels, reveals modifications to a few of the peaks. Minor deformations are discernible in the bands of  $2916.21\text{ cm}^{-1}$  upon comparing the biomass with the solid product of ratio 1:10. This could be the result of cellulose and hemicellulose's C-H bonds breaking down. A similar variation is seen in ratio 1:50 signal, but with a more pointed peak. Dehydration during the hydrothermal process may be the cause of the peak's broadening at  $3334.21\text{ cm}^{-1}$  [49]. Conversely, the bands located at  $1704.48$ ,  $1603.91$ , and approximately  $832.12\text{ cm}^{-1}$  appeared to be more intense than the unaltered biomass; based on the literature, these peaks support a modification in the cellulose and hemicellulose structures, potentially as a result of degradation reactions. The experiment's bands of  $1513.11$ ,  $1427.09$ ,  $1204.38$ , and  $1158.91$  present a greater modification, mainly in the 1:50 ratio, compared to the unmodified biomass.

The peaks mentioned above are mainly associated with cellulose and hemicellulose, so it is inferred that degradation of these biopolymers occurs under HTC conditions [19]. As for the  $1453.05\text{ cm}^{-1}$  band, this peak is characteristic of lignin, so being sharper, it can be deduced that a possible lignin hydrolysis occurs. The band of  $1315.47\text{ cm}^{-1}$  disappears with the increase in the variation of the B:W ratio during the HTC reaction. Also, at the band of  $1204.38\text{ cm}^{-1}$ , the formation of a shoulder is evident. This is characteristic of the deformation of primary alcohols and the C-O stretching of the ether bond in lignin [43,47].

### The Morphology of the Samples Microscopically

SEM is used to observe the morphology of the samples microscopically. Figure 6 shows the photographs of the 12 hydrocarbons obtained and compares them according to the variation of particle size and B:W ratio. The morphology of sugarcane bagasse before treatment is characterized by having a fibrous and compact structure [50]. First, when comparing the hydrocarbons obtained by varying the particle sizes and maintaining the same operating conditions (B:W ratio and temperature), it was observed that when particle sizes were increased from 106 to 600  $\mu\text{m}$ , hydrocarbons with more cracks and pores on the surface of the solid material were produced. It was also observed that most of the solids obtained at 260  $^{\circ}\text{C}$  had a more porous surface with respect to those at 220  $^{\circ}\text{C}$ . In addition, in the photographs of hydrocarbons 2, 6, and 10, some solid structures were identified. As reported in the literature, this may be due to a modification in the surface characteristics of the material during HTC conversion because chemical changes occur in the lignocellulosic structural composition of the biomass. Likewise, at high temperatures, mechanisms of polymerization of the monomers that constitute the lignocellulose and degradation of the compounds present in the aqueous phase have been associated with the formation of products with a high carbon content and a morphology similar to a microsphere [51,52].

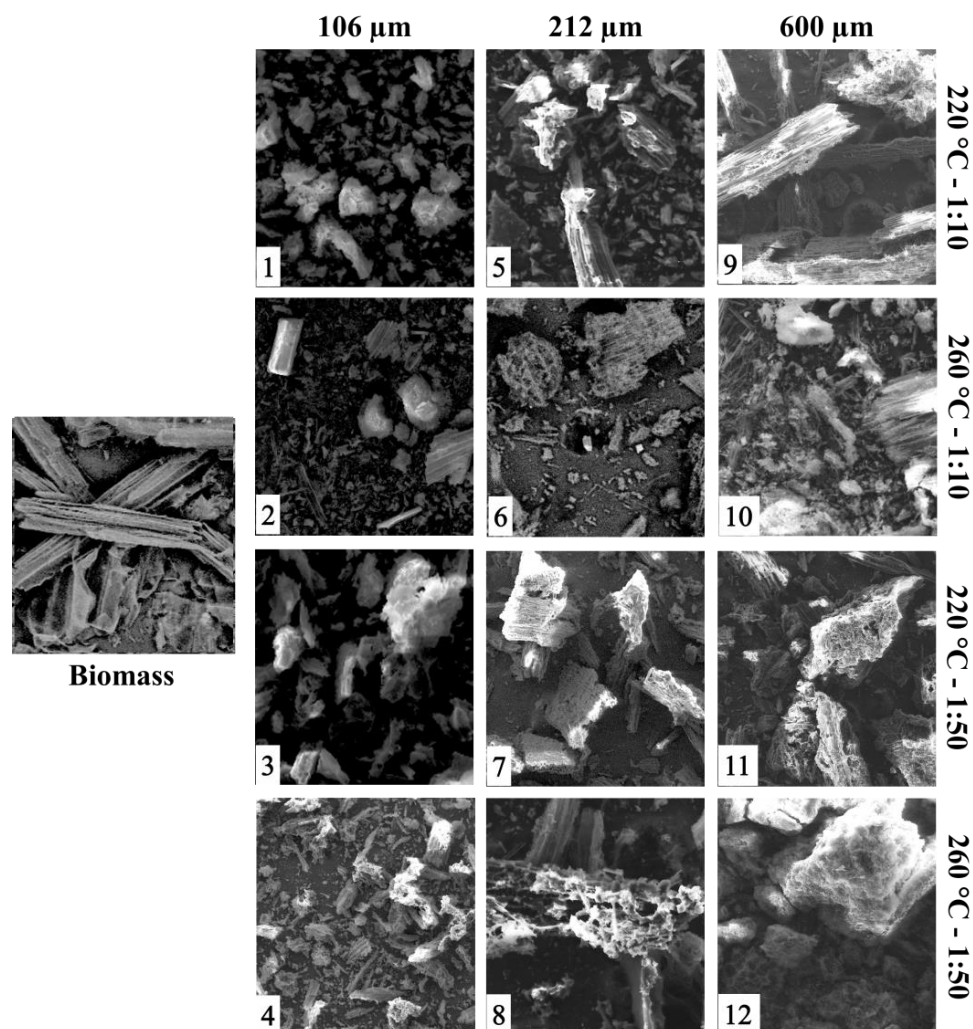


**Figure 6.** SEM photographs of hydrocarbons, compared by particle size.

With respect to the variation in the proportions of biomass to water within the reaction system, it was observed that the hydrocarbons obtained from the proportions 1:50 were characterized by having a surface with more porosities and cracks compared to those

obtained in the proportions 1:10. This may be due to the characteristics of sugarcane bagasse, remembering that given its medullary and fibrovascular structure, it has the capacity to absorb and retain water. For this reason, a greater amount of water guarantees better heat and mass transfer in the reaction medium [50].

#### Elemental Analysis

From the information provided in Table 6, it could be observed that the biomass conversion using HTC treatment generated a greater amount of solid products when the working temperature was 260 °C. In the table, these data correspond to rows 2, 4, 6, 8, 10, and 12. It was observed that the operating conditions of experiment 8 showed the best percentage of solid product conversion on a dry basis (85.851%), and the operating conditions were: reaction temperature of 260 °C, 212 µm particle size, and a B:A ratio of 1:50.

**Table 6.** Elemental composition EDX-SEM of the hydrochars.

Experiment Number	%				Conversion by Weight of Solid Product	O/C
	C	O	N	Other		
Biomass	44.22	45.56	0.292			1.030
1	68.605	25.655	5.140	Si = 0.39; F = 0.21	49.592	0.375
2	70.255	20.335	68.605	Si = 4.76	59.132	0.297
3	61.965	33.165	4.420	F = 0.45	52.921	0.536
4	77.565	15.975	6.465		72.187	0.206
5	68.520	25.890	5.465	Si = 0.12	56.712	0.380
6	74.920	10.730	3.650		58.490	0.142
7	64.110	27.330	9.235		65.860	0.426
8	74.310	19.540	6.150		85.851	0.263
9	67.540	27.345	5.115		51.196	0.405
10	74.180	19.570	6.250		62.759	0.264
11	63.200	31.825	4.985		57.454	0.504
12	75.865	17.910	6.225		74.213	0.236

Regarding elemental composition, it was observed that %C and %N of hydrocarbons increased compared to the original biomass, while %O decreased. When evaluating the O/C ratio, a decrease in the O/C ratio was observed. According to the Van Krevelen diagrams, it can be inferred that the material is carbonizing and is losing oxygen. Therefore, hydrocarbons obtained at higher temperatures have an O/C ratio similar to that of lignite [53].

#### 4. Conclusions

According to the results obtained, it can be inferred that the conditions that can favor the formation of platform chemicals are: experiment 7, 220 °C, 212 µm, B:W 1:50. Similarly, the solid phase was monitored using IR spectroscopy, which showed that at 260 °C, the structural composition of the sugarcane bagasse showed a greater degradation of the lignocellulosic components. The B:W ratio had a greater effect on the decomposition pattern when using the 1:50 ratio, while when evaluating the effect on particle size, it is evident that this parameter has a different tendency for each of the biomass and water ratios.

By using HPLC-RI chromatographic analysis, it was determined that the most appropriate conditions for obtaining platform chemicals were at a biomass-to-water ratio 1:50, temperature 220 °C, and particle size 212 µm, for a yield of 31.073%. The platform chemicals identified in the aqueous fractions were carbohydrates (glucose, xylose), formic acid, levulinic acid, HMF, and furfural. Formic acid was the platform chemical with the highest yield, 15.926% by weight on a dry basis. Regarding the solid product, it was evidenced that the hydrocarbons that presented greater porosities and cracks on the surface of the solid were those obtained from the biomass at a size of 600 µm, with a reaction temperature of

260 °C, and with a B:A ratio of 1:50. In the elemental composition of the hydrocarbons, it was evidenced that the carbon content increased compared to the untreated biomass while the amount of oxygen decreased. By observing the decrease in the O/C ratio, it can be inferred that, through different reaction mechanisms, the solid products are carbonizing.

**Author Contributions:** Conceptualization, L.N.M.-C.; methodology, L.N.M.-C. and A.S.L.-P.; validation, L.N.M.-C. and A.S.L.-P.; formal analysis L.N.M.-C. and A.S.L.-P.; investigation, L.N.M.-C. and A.S.L.-P.; resources, C.A.G.-F.; data curation, L.N.M.-C. and A.S.L.-P.; writing—original draft preparation, L.N.M.-C. and A.S.L.-P.; writing—review and editing, C.A.G.-F.; supervision, C.A.G.-F.; project administration, C.A.G.-F.; funding acquisition, A.S.L.-P. All authors have read and agreed to the published version of the manuscript.

**Funding:** This research was funded by MINCIENCIAS, Contrato de financiamiento de recuperación contingente No. 80740-101-2022.

**Data Availability Statement:** Data are contained within the article.

**Acknowledgments:** We thank the Universidad Nacional de Colombia and the Departamento de Química for their support and the possibility of using the equipment and techniques that allowed for the development of this article.

**Conflicts of Interest:** The authors declare no conflicts of interest.

## References

1. FINAGRO. Crecimiento del Sector Agropecuario y AgroExpo 2023, un Reto Hacia el Desarrollo del Campo | Finagro. Available online: <https://www.finagro.com.co/noticias/articulos/crecimiento-del-sector-agropecuario-agroexpo-2023-reto-desarrollo-del-campo-0> (accessed on 7 December 2023).
2. DANE. Boletín Encuesta Nacional Agropecuaria 2019. DANE. Available online: <https://www.dane.gov.co/index.php/estadisticas-por-tema/agropecuario/encuesta-nacional-agropecuaria-ena> (accessed on 7 December 2023).
3. DANE. DANE—PIB Información Técnica. DANE. Available online: <https://www.dane.gov.co/index.php/estadisticas-por-tema/cuentas-nacionales/cuentas-nacionales-trimestrales/pib-informacion-tecnica> (accessed on 7 November 2021).
4. DANE. Boletín mensual Insumos y Factores Asociados a la Producción Agropecuaria. 2020. Available online: <http://www.agronet.gov.co/> (accessed on 6 November 2021).
5. DANE. Un Camino para la Inclusión, la Equidad y el Reconocimiento. Available online: [https://www.mineducacion.gov.co/1759/articles-362822\\_recurso.pdf](https://www.mineducacion.gov.co/1759/articles-362822_recurso.pdf) (accessed on 8 December 2023).
6. Felipe, J.; Bustamante, L. *La Caña de Azúcar (Saccharum officinarum) para la Producción de Panela. Caso: Nordeste del Departamento de Antioquia*; National Open and Distance University UNAD: Bogotá, Colombia, 2015.
7. Minagricultura. Cadena Agroindustrial de la Panela. Colombia, 2019. Available online: <https://sioc.minagricultura.gov.co/Panela/Documentos/2019-12-30%20Cifras%20Sectoriales.pdf> (accessed on 2 January 2022).
8. Kambo, H.S.; Dutta, A. A comparative review of biochar and hydrochar in terms of production, physico-chemical properties and applications. *Renew. Sustain. Energy Rev.* **2015**, *45*, 359–378. [CrossRef]
9. Peterson, A.A.; Vogel, F.; Lachance, R.P.; Fröling, M.; Antal, M.J., Jr.; Tester, J.W. Thermochemical biofuel production in hydrothermal media: A review of sub- and supercritical water technologies. *Energy Environ. Sci.* **2008**, *1*, 32. [CrossRef]
10. Shen, Y. A review on hydrothermal carbonization of biomass and plastic wastes to energy products. *Biomass Bioenergy* **2020**, *134*, 105479. [CrossRef]
11. Zhuang, X.; Zhan, H.; Song, Y.; He, C.; Huang, Y.; Yin, X.; Wu, C. Insights into the evolution of chemical structures in lignocellulose and non-lignocellulose biowastes during hydrothermal carbonization (HTC). *Fuel* **2019**, *236*, 960–974. [CrossRef]
12. Coronella, C.J.; Lynam, J.G.; Reza, M.T.; Uddin, M.H. Hydrothermal Carbonization of Lignocellulosic Biomass. In *Application of Hydrothermal Reactions to Biomass Conversion*; Springer: Berlin/Heidelberg, Germany, 2014; pp. 275–311. [CrossRef]
13. Heidari, M.; Dutta, A.; Acharya, B.; Mahmud, S. A review of the current knowledge and challenges of hydrothermal carbonization for biomass conversion. *J. Energy Inst.* **2019**, *92*, 1779–1799. [CrossRef]
14. Nguyen, T.A.H.; Bui, T.H.; Guo, W.S.; Ngo, H.H. Valorization of the aqueous phase from hydrothermal carbonization of different feedstocks: Challenges and perspectives. *Chem. Eng. J.* **2023**, *472*, 144802. [CrossRef]
15. Fang, J.; Zhan, L.; Ok, Y.S.; Gao, B. Minireview of potential applications of hydrochar derived from hydrothermal carbonization of biomass. *J. Ind. Eng. Chem.* **2018**, *57*, 15–21. [CrossRef]
16. Rehman, A.; Nazir, G.; Heo, K.; Hussain, S.; Ikram, M.; Akhter, Z.; Algaradah, M.M.; Mahmood, Q.; Fouda, A.M. A focused review on lignocellulosic biomass-derived porous carbons for effective pharmaceuticals removal: Current trends, challenges and future prospects. *Sep. Purif. Technol.* **2024**, *330*, 125356. [CrossRef]
17. Onokwai, A.O.; Ajisegiri, E.S.A.; Okokpujie, I.P.; Ibikunle, R.A.; Oki, M.; Dirisu, J.O. Characterization of lignocellulose biomass based on proximate, ultimate, structural composition, and thermal analysis. *Mater. Today Proc.* **2022**, *65*, 2156–2162. [CrossRef]

18. Edreis, E.M.A.; Luo, G.; Yao, H. Investigations of the structure and thermal kinetic analysis of sugarcane bagasse char during non-isothermal CO<sub>2</sub> gasification. *J. Anal. Appl. Pyrolysis* **2014**, *107*, 107–115. [CrossRef]
19. Castro Vega, A.A. Estudio de la Naturaleza Química de Biocrudos Obtenidos Mediante Licuefacción Hidrotérmica de Biomasa Lignocelulósica. 2011. Available online: <https://repositorio.unal.edu.co/handle/unal/8651> (accessed on 8 December 2023).
20. Castro, A.A.V.; Varela, L.I.R.; Díaz Velásquez, J. Subcritical hydrothermal conversion of organic wastes and biomass. Reaction pathways. *Ing. E Investig.* **2007**, *27*, 41–50. [CrossRef]
21. Qian, C.; Li, Q.; Zhang, Z.; Wang, X.; Hu, J.; Cao, W. Prediction of higher heating values of biochar from proximate and ultimate analysis. *Fuel* **2020**, *265*, 116925. [CrossRef]
22. *Preparation of Samples for Compositional Analysis*; Technical Report NREL/TP-510-42620; National Renewable Energy Laboratory: Golden, CO, USA, 2008. Available online: <https://www.nrel.gov/docs/gen/fy08/42620.pdf> (accessed on 7 December 2023).
23. *Determination of Total Solids in Biomass and Total Dissolved Solids in Liquid Process Samples*; Technical Report NREL/TP-510-42621; National Renewable Energy Laboratory: Golden, CO, USA, 2008. Available online: <https://www.nrel.gov/docs/gen/fy08/42621.pdf> (accessed on 7 December 2013).
24. *Determination of Ash in Biomass*; (NREL/TP-510-42622); National Renewable Energy Laboratory: Golden, CO, USA, 2008. Available online: <https://www.nrel.gov/docs/gen/fy08/42622.pdf> (accessed on 7 December 2023).
25. *Standard Test Method for Volatile Matter in the Analysis of Particulate Wood Fuels (ASTM E872-82(2019))*; ASTM International: West Conshohocken, PA, USA, 2019. Available online: <https://www.astm.org/e0872-82r19.html> (accessed on 7 December 2023).
26. *Standard Test Methods for Determination of Carbon, Hydrogen and Nitrogen in Analysis Samples of Coal and Carbon in Analysis Samples of Coal and Coke (ASTM D5373-21)*. 2021. Available online: <https://www.astm.org/d5373-21.html> (accessed on 7 December 2023).
27. Fiber (Acid Detergent) and Lignin (H<sub>2</sub>SO<sub>4</sub>) in Animal Feed. In *AOAC (AOAC 973.18-1977)*; AOAC: Rockville, MD, USA, 2021; Available online: [http://www.aocofficialmethod.org/index.php?main\\_page=product\\_info&products\\_id=1165](http://www.aocofficialmethod.org/index.php?main_page=product_info&products_id=1165) (accessed on 7 December 2023).
28. Van Soest, P.; Robertson, J.B.; Lewis, B.A. Methods for dietary fiber, neutral detergent fiber, and nonstarch polysaccharides in relation to animal nutrition. *J. Dairy Sci.* **1991**, *74*, 3583–3597. [CrossRef] [PubMed]
29. Ayeni, A.O.; Adeyo, O.A.; Oresegun, O.M.; Oladimeji, T.E. Compositional analysis of lignocellulosic materials: Evaluation of an economically viable method suitable for woody and non-woody biomass. *Am. J. Eng. Res.* **2015**, *4*, 14–19. Available online: <https://www.ajer.org> (accessed on 14 January 2024).
30. Onokwai, A.O.; Okokpujie, I.P.; Ajisegiri, E.S.; Oki, M.; Adeoyeb, A.O.; Akinlabi, E.T. Characterization of Lignocellulosic Biomass Samples in Omu-Aran Metropolis, Kwara State, Nigeria, as Potential Fuel for Pyrolysis Yields. *Int. J. Renew. Energy Dev.* **2022**, *11*, 973–981. [CrossRef]
31. Hincapié, G.; Soto, A.; López, D. Pre-tratamiento ácido y básico de bagazo de caña y de compuestos modelo para la producción de bio-aceite vía licuefacción hidrotérmica. *Energética* **2016**, *47*, 23–30. Available online: <https://repositorio.unal.edu.co/handle/unal/64263> (accessed on 14 January 2024).
32. Zhang, P.; Liao, W.; Kumar, A.; Zhang, Q.; Ma, H. Characterization of sugarcane bagasse ash as a potential supplementary cementitious material: Comparison with coal combustion fly ash. *J. Clean. Prod.* **2020**, *277*, 123834. [CrossRef]
33. Khatami, R.; Stivers, C.; Joshi, K.; Levendis, Y.A.; Sarofim, A.F. Combustion behavior of single particles from three different coal ranks and from sugarcane bagasse in O<sub>2</sub>/N<sub>2</sub> and O<sub>2</sub>/CO<sub>2</sub> atmospheres. *Combust. Flame* **2012**, *159*, 1253–1271. [CrossRef]
34. Yao, S.; Nie, S.; Yuan, Y.; Wang, S.; Qin, C. Efficient extraction of bagasse hemicelluloses and characterization of solid remainder. *Bioresour. Technol.* **2015**, *185*, 21–27. [CrossRef]
35. Wüst, D.; Correa, C.R.; Jung, D.; Zimmermann, M.; Kruse, A.; Fiori, L. Understanding the influence of biomass particle size and reaction medium on the formation pathways of hydrochar. *Biomass Convers. Biorefin.* **2020**, *10*, 1357–1380. [CrossRef]
36. Heidari, M.; Salaudeen, S.; Dutta, A.; Acharya, B. Effects of Process Water Recycling and Particle Sizes on Hydrothermal Carbonization of Biomass. *Energy Fuels* **2018**, *32*, 11576–11586. [CrossRef]
37. Zhou, Y.; Remón, J.; Pang, X.; Jiang, Z.; Liu, H.; Ding, W. Hydrothermal conversion of biomass to fuels, chemicals and materials: A review holistically connecting product properties and marketable applications. *Sci. Total Environ.* **2023**, *886*, 163920. [CrossRef] [PubMed]
38. Usman, M.; Chen, H.; Chen, K.; Ren, S.; Clark, J.H.; Fan, J.; Luo, G.; Zhang, S. Characterization and utilization of aqueous products from hydrothermal conversion of biomass for bio-oil and hydro-char production: A review. *Green. Chem.* **2019**, *21*, 1553–1572. [CrossRef]
39. Zhou, Y.; Li, M.; Chen, Y.; Hu, C. Conversion of polysaccharides in *Ulva prolifera* to valuable chemicals in the presence of formic acid. *J. Appl. Phycol.* **2021**, *33*, 101–110. [CrossRef]
40. Krysanova, K.; Krylova, A.; Kulikova, M.; Kulikov, A.; Rusakova, O. Biochar characteristics produced via hydrothermal carbonization and torrefaction of peat and sawdust. *Fuel* **2022**, *328*, 125220. [CrossRef]
41. Zhu, R.; Yadama, V. Effects of hot water extraction pretreatment on physicochemical changes of Douglas fir. *Biomass Bioenergy* **2016**, *90*, 78–89. [CrossRef]
42. Sabry, T.M.; El-Korashy, S.A.E.-H.; Jahin, H.E.S.; Khairy, G.M.; Aal, N.F.A. Hydrothermal carbonization of *Calotropis procera* leaves as a biomass: Preparation and characterization. *J. Mol. Struct.* **2024**, *1302*, 137397. [CrossRef]

43. Sevilla, M.; Fuertes, A.B. The production of carbon materials by hydrothermal carbonization of cellulose. *Carbon*. N. Y. **2009**, *47*, 2281–2289. [[CrossRef](#)]
44. Ju, Y.H.; Huynh, L.H.; Kasim, N.S.; Guo, T.J.; Wang, J.H.; Fazary, A.E. Analysis of soluble and insoluble fractions of alkali and subcritical water treated sugarcane bagasse. *Carbohydr. Polym.* **2011**, *83*, 591–599. [[CrossRef](#)]
45. Iryani, D.A.; Kumagai, S.; Nonaka, M.; Sasaki, K.; Hirajima, T. Characterization and Production of Solid Biofuel from Sugarcane Bagasse by Hydrothermal Carbonization. *Waste Biomass Valorization* **2017**, *8*, 1941–1951. [[CrossRef](#)]
46. Nicolae, S.A.; Au, H.; Modugno, P.; Luo, H.; Szego, A.E.; Qiao, M.; Li, L.; Yin, W.; Heeres, H.J.; Berge, N.D.; et al. Recent advances in hydrothermal carbonisation: From tailored carbon materials and biochemicals to applications and bioenergy. *Green. Chem.* **2020**, *22*, 4747–4800. [[CrossRef](#)]
47. Kozarski, M.; Klaus, A.; Nikšić, M.; Van Griensven, L.J.L.D.; Vrvic, M.M.; Jakovljević, D. Polysaccharides of higher fungi: Biological role, structure, and antioxidative activity. *Hemijaska Industrija* **2014**, *68*, 305–320. [[CrossRef](#)]
48. Никоненко, Н.А.; Buslov, D.K.; Sushko, N.I.; Zhbankov, R.G. Spectroscopic manifestation of stretching vibrations of glycosidic linkage in polysaccharides. *J. Mol. Struct.* **2005**, *752*, 20–24. [[CrossRef](#)]
49. Nikonenko, N.A.; Buslov, D.K.; Sushko, N.I.; Zhbankov, R.G. Investigation of stretching vibrations of glycosidic linkages in disaccharides and polysaccharides with use of IR spectra deconvolution. *Biopolym. Orig. Res. Biomol.* **2000**, *57*, 257–262. [[CrossRef](#)]
50. Thite, V.S.; Nerurkar, A.S. Valorization of sugarcane bagasse by chemical pretreatment and enzyme mediated deconstruction. *Sci. Rep.* **2019**, *9*. [[CrossRef](#)] [[PubMed](#)]
51. Corrales, R.C.N.R.; De Souza Nogueira Sardinha Mendes, F.; Perrone, C.C.; Sant’Anna, C.; De Souza, W.; Abud, Y.; Bon, E.P.S.; Ferreira-Leitão, V.S. Structural evaluation of sugar cane bagasse steam pretreated in the presence of CO<sub>2</sub> and SO<sub>2</sub>. *Biotechnol. Biofuels* **2012**, *5*. [[CrossRef](#)] [[PubMed](#)]
52. Ibbett, R.; Gaddipati, S.; Davies, S.M.; Hill, S.E.; Tucker, G.A. The mechanisms of hydrothermal deconstruction of lignocellulose: New insights from thermal–analytical and complementary studies. *Bioresour. Technol.* **2011**, *102*, 9272–9278. [[CrossRef](#)]
53. Santín, C.; Doerr, S.H.; Merino, A.; Bucheli, T.D.; Bryant, R.; Ascough, P.; Gao, X.; Masiello, C.A. Carbon sequestration potential and physicochemical properties differ between wildfire charcoals and slow-pyrolysis biochars. *Sci. Rep.* **2017**, *7*, 11233. [[CrossRef](#)]

**Disclaimer/Publisher’s Note:** The statements, opinions and data contained in all publications are solely those of the individual author(s) and contributor(s) and not of MDPI and/or the editor(s). MDPI and/or the editor(s) disclaim responsibility for any injury to people or property resulting from any ideas, methods, instructions or products referred to in the content.